Distinct Firing Properties of Higher Order Thalamic Relay Neurons

Jianli Li,[1] **Martha E. Bickford,**[1] **and William Guido**[2]

[1]*Department of Anatomical Sciences and Neurobiology, University of Louisville, Louisville, Kentucky 40292; and* [2]*Department of Cell Biology and Anatomy, Louisiana Health Sciences Center, New Orleans, Louisiana 70112*

Li, Jianli, Martha E. Bickford, and William Guido. Distinct firing properties of higher order thalamic relay neurons. *J Neurophysiol* 90: 291–299, 2003. First published March 12, 2003; 10.1152/jn.01163.2002. It has been proposed that the thalamus is composed of at least two types of nuclei. First-order relay nuclei transmit signals from the periphery to the cortex while higher order nuclei may route information from one cortical area to another. Although much is known about the functional properties of relay neurons in first-order nuclei, little is known about relay neurons belonging to higher-order nuclei. We investigated the electrophysiological properties of relay cells in a higher-order thalamic nucleus using in vitro intracellular recordings from thalamic slices of the rat's lateral posterior nucleus (LPN). We found neurons of the LPN possess many of the same membrane properties as first-order relay neurons. These included low-threshold calcium spikes (I_T) and burst firing, a mixed cation conductance (I_H) that prevented membrane hyperpolarization, and a transient K^+ conductance that delayed spike firing (I_A). The repetitive firing characteristics of LPN neurons were more distinct. One group of cells, located in the more caudal regions of the LPN responded to depolarizing current pulses with a train of action potentials or in a regular spiking (RS) mode. This form of firing showed a steep but highly linear increase in firing frequency with increasing levels of membrane depolarization. Another group of cells, located in the more rostral regions of the LPN, responded to depolarizing current pulses with clusters of high-frequency bursts or in a clustered spiking (CS) mode. The overall firing frequency rose nonlinearly with membrane depolarization, but the frequency of a given burst remained relatively constant. The caudal LPN receives input from the superior colliculus, whereas the rostral LPN receives input from layers V and VI of the visual cortex. Thus the RS and CS cells may be driven by subcortical and cortical inputs respectively, and the distinct temporal properties of their response modes may be a necessary component of the LPN circuitry.

INTRODUCTION

It has been proposed that nuclei of the dorsal thalamus can be divided into two general types. First-order nuclei convey sensory information to the cortex, while higher-order nuclei may contribute to the transfer of information from one cortical area to another (Guillery and Sherman 2002). Although anatomical distinctions between these nuclei are well established, there has been little attention given to the possibility that cells in these nuclei possess different functional properties.

Much is known about the electrophysiological properties and firing characteristics of first-order neurons, such as thalamocortical (relay) cells in the dorsal lateral geniculate nucleus (LGN). These cells transmit retinal signals to the visual cortex by means of single spike (tonic) or burst firing response modes (McCormick and Feeser 1990; Sherman 2001; Steriade and Llinás 1988). Tonic firing prevails at depolarized membrane levels and ensures a relatively accurate transfer of retinal signals. Burst firing, a high-frequency barrage of action potentials that ride the peak of a low-threshold Ca^{2+} spike, occurs at more hyperpolarized levels and introduces a highly nonlinear form of signaling. Burst and tonic modes play a key role in thalamic signaling and underscore how first-order relay neurons actively modulate the gain and efficacy of signal transmission. However, few studies have explored the firing modes and intrinsic membrane properties of higher-order relay cells (Hu 1993; Monckton and McCormick 2002; Zhu and Heggelund 2001). To examine the electrophysiological properties of cells in a higher-order thalamic nucleus, we made in vitro intracellular recordings of relay cells in the rat lateral posterior nucleus (LPN).

The LPN receives visual input from the retinorecipient zone of the superior colliculus as well as the visual cortex (Li and Bickford 2001; Li et al. 2003; Mason and Groos 1981; Takahashi 1985). The LPN is considered a higher-order nucleus because it is innervated by two different types of cortical terminals that originate in layers V and VI (Bourassa and Deschênes 1995; Guillery 1995; Li et al. 2003). It has been proposed that higher-order thalamic neurons are distinct from first order thalamic neurons because their response properties may be driven by cortical rather than subcortical inputs (Guillery 1995).

METHODS

Long Evans rats ranging in age from postnatal day 18–47 were anesthetized with halothane and killed by decapitation. The brain was excised and a block of tissue containing the thalamus was removed, and placed in a cold (4°C) oxygenated solution of artificial cerebrospinal fluid (ACSF) containing (in mM) 124 NaCl, 2.5 KCl, 2 $CaCl_2$, 1 $MgSO_4$, 26 NaH_2PO_4, and 10 dextrose at a pH of 7.4. Thalamic slices were prepared on a vibratome (Leica, VT 1000E, Deerfield, IL) as 400-μm-thick coronal or parasagittal sections. Slices were placed on nylon mesh designed to fit inside a well of a temperature controlled recording chamber (Fine Science Tools, Foster City, CA). Tissue was maintained in an interface of warmed (35°C) humidified air (95% O_2-5% CO_2) and oxygenated ACSF. Recordings began 2 h after slices were placed in the recording chamber.

Examples of thalamic slices containing the LPN and our basic experimental approach are shown in Fig. 1. We used coronal or
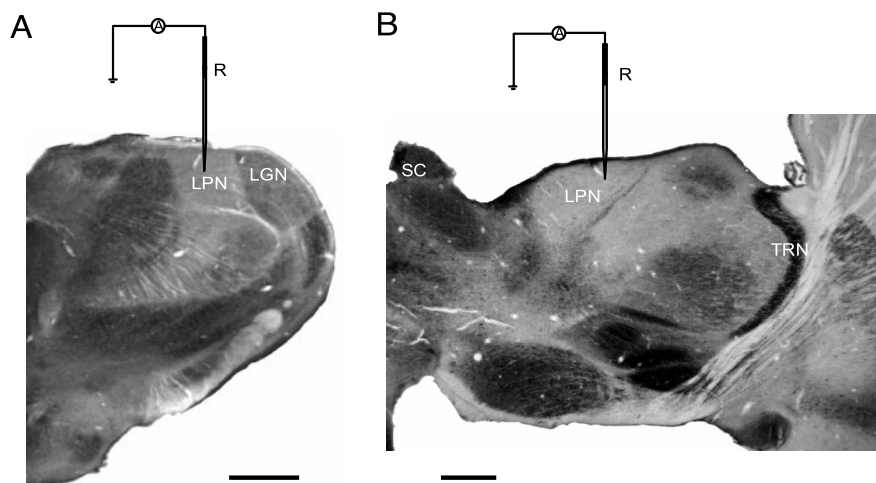
FIG. 1. Examples of thalamic slices and basic experimental approach. Recording sites are illustrated in a coronal (*A*) and a parasagittal section (*B*) labeled by an antibody against parvalbumin. Scale bars in *A* and *B* = 1 mm. LPN, lateral posterior nucleus; LGN, lateral geniculate nucleus; SC, superior colliculus.

parasaggittal slices to obtain intracellular recordings from neurons within the LPN. Sharp-tipped electrodes made of borosilicate glass (Sutter Instruments, Novato, CA) and filled with 4 M KAC or a 2% solution of biocytin dissolved in 2 M KAC were used to record intracellular voltage responses. Electrodes were pulled horizontally (P97, Sutter Instruments) to a final impedance of 60–120 MΩ. Intracellular responses were collected in current-clamp mode with a high-impedance amplifier (Axoclamp 2B, Axon Instruments, Union City, CA) using techniques described elsewhere (Guido et al. 1997, 1998). Neuronal activity was digitized at 10 kHz (Instrutech VR10B, Port Washington, NY) and stored directly on computer. Current and voltage data were acquired and analyzed using pulse and pulsefit (HEKA, Port Washington, NY) software programs. Adjustments in membrane potential were controlled by injecting DC current through the recording electrode. Current-voltage relations were examined at different membrane potentials by injecting a series of square wave current pulses (±1 nA, 0.01- to 0.1-nA steps, 300–700 ms) to reach steady state. The voltage responses to these current steps were also used to determine the presence and operating range of voltage gated conductances and to explore the repetitive firing characteristics of LPN cells. In some instances, the K$^+$ channel blockers apamin (250–500 μM) tetraethylammonium (TEA; 10 mM) or 4-aminopiridine (4-AP, 500 μM to 1 mM) were applied locally into the interface recording chamber. In other experiments, NiCl$_2$ (1–2 mM) or CsCl (2 mM) were added to the bath.

During intracellular recording, some LPN neurons (*n* = 51) were filled with biocytin by passing alternating positive and negative current pulses (±1 nA, 30 ms, 100–300 pulses) through the recording electrode. Slices containing biocytin filled cells were placed in a fixative solution of 4% paraformaldehyde in 0.1 M phosphate buffer (PB) for 48 h and processed using the ABC method (Guido et al. 1997; Horikawa and Armstrong 1988). Labeled cells were photographed and drawn using a camera lucida attachment. Soma sizes were measured using a digitizing tablet and SigmaScan software (SPSS, Chicago, IL).

To stain cells in the LPN that contained gamma amino butyric acid (GABA), two rats were deeply anesthetized with pentobarbital sodium (30 mg/kg) and perfused through the heart with tyrode solution followed by a fixative solution of 4% paraformaldehyde and 1% glutaraldehyde in PB. The brain was removed and 50-μm-thick sections were cut with a vibratome. The sections were incubated overnight in a 1:4,000 dilution of a rabbit-anti-GABA antibody (Sigma Chemical, St. Louis, MO). The next day the sections were incubated in a biotinylated goat-anti rabbit antibody for 1 h, ABC for 1 h, and reacted with nickel enhanced diaminobenzidine. GABA stained somata were drawn and measured as described in the preceding text.

To illustrate the boundaries of the LPN, two rats were perfused with tyrode solution followed by a fixative solution of 4% paraformalde-

hyde in PB. The brain was removed and 50-μm-thick sections were cut on a vibratome. The sections were incubated overnight in a 1:3,000 dilution of a mouse-anti-parvalbumin antibody (Sigma). The next day the sections were incubated in a biotinylated goat-anti mouse antibody for 1 h, ABC for 1 h, and reacted with nickel enhanced diaminobenzidine.

RESULTS

We recorded the voltage responses of 94 neurons in the LPN. Of these, 51 were filled with biocytin. Examples of biocytin-filled cells are shown in Figs. 2*B* and 8. The soma size distribution in Fig. 2*C* indicates that all labeled cells were larger than those stained for GABA (Fig. 2*A*), a neurotransmitter used by thalamic interneurons (Montero and Zempel 1985). Biocytin-labeled cells in the LPN also had multipolar dendritic arbors consistent with those of class A thalamocortical cells (Grossman et al. 1973; Webster and Rowe 1984). Taken together, these results indicate our recordings were made from thalamic relay cells.

Intrinsic membrane properties of LPN cells

The voltage responses to square-wave current pulses were used to explore the passive and active membrane properties of LPN relay neurons. Examples are shown in Figs. 2–5. Measurements of these responses revealed that input resistance (55 ± 19MΩ; *n* = 94), resting membrane potential (−60 ± 4 mV; *n* = 67), and spike amplitude (64 ± 7mV; *n* = 80) are similar to those of LGN relay neurons (Williams et al. 1996). An examination of *I-V* relations also indicated substantial nonlinearities in the voltage responses to current pulses (Fig. 2*E*). Indeed, LPN cells possessed many of the same voltage-gated conductances found in first-order relay neurons (McCormick 1992; Williams et al. 1996). This included delayed firing in response to depolarizing current pulses (Fig. 2*D*, a), and a hyperpolarization-activated depolarization (Fig. 2*D*, b) and rebound burst firing (Fig. 2*D*, c) in response to hyperpolarizing current pulses.

All recorded LPN cells displayed a low-threshold (LT) T-type Ca^{2+} conductance. Activation gave rise to a large triangular depolarization and burst firing at hyperpolarized membrane potentials. Passive membrane repolarization on termination of a hyperpolarizing current pulse of sufficient strength
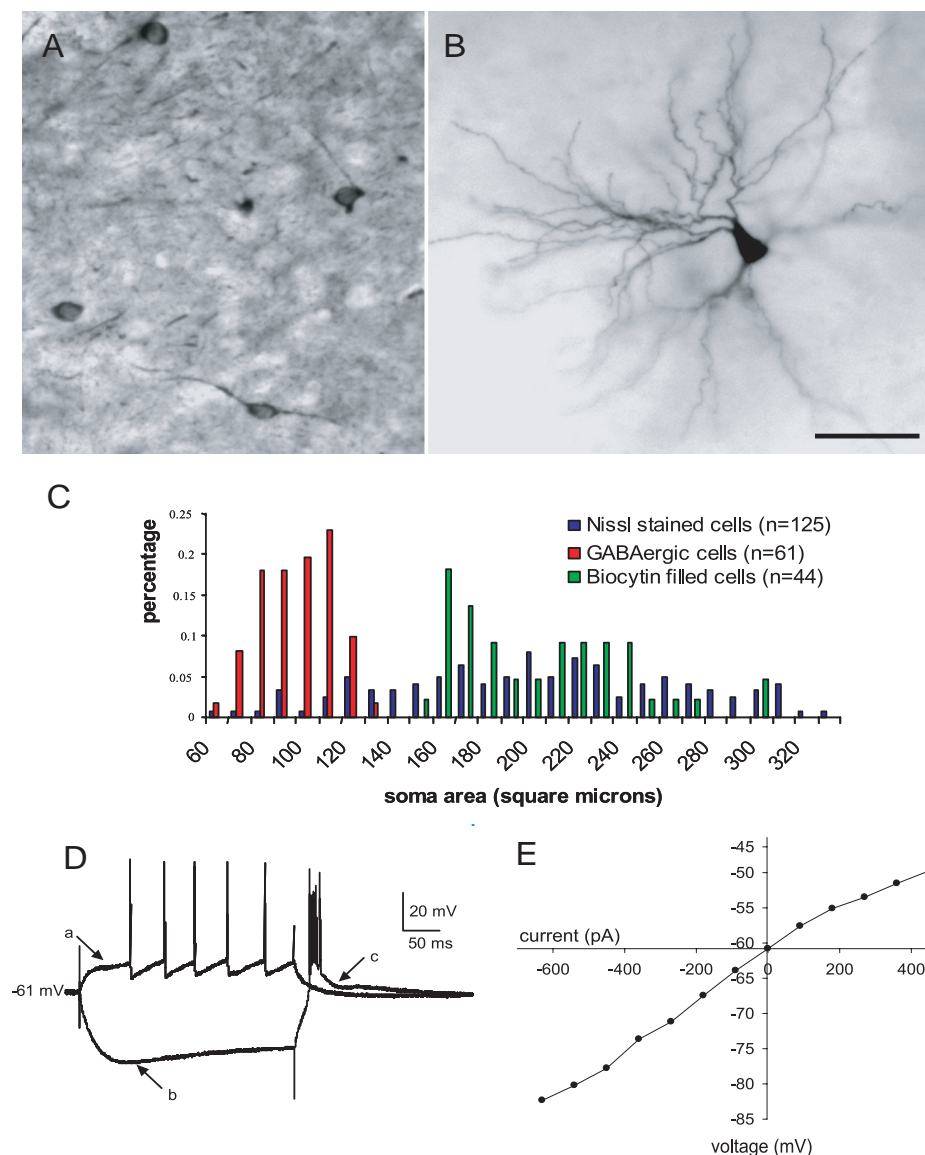
FIG. 2. Morphology and electrophysiological properties of LPN relay cells. *A*: a photograph of the LPN showing cells stained for gamma amino butyric acid (GABA). *B*: a photograph of an LPN cell filled with biocytin following intracellular recording. *C*: a histogram showing the distribution of soma sizes in the LPN stained for Nissl substance, GABA, or by intracellular injection of biocytin. All biocytin filled neurons were larger than GABAergic interneurons. Scale bar in *B* = 50 μm and applies to *A* and *B*. *D*: examples of the voltages responses of the LPN cell relay cell shown in *B*. Depolarization produces an outward rectification (a) that delays spike firing. Membrane hyperpolarization produces a strong inward rectification (b). Passive repolarization from a hyperpolarized state activates a rebound low-threshold Ca^{2+} spike and burst firing (c). *E*: corresponding *I-V* plot derived from voltage responses as shown in *D* to a series of square-wave current pulses (±1 nA, 0.1-nA steps, 320 ms).

and duration evoked large "rebound" LT spikes and burst firing. These events were also activated by a depolarization from a steady hyperpolarized state (see Fig. 5). LT spikes could be blocked by bath application of Ni^{2+} ($n = 3$, data not shown), indicating they are mediated by a T-type Ca^{2+} channel (I_T) (Hernandez-Cruz and Pape 1989).

LPN neurons (54/55) also displayed a hyperpolarization-activated depolarization. As shown in Fig. 3, *A* and *B,* hyperpolarizing current pulses produced a strong inward rectifying response. This "depolarizing sag" was blocked by bath application of Cs$^+$ ($n = 3$), thus indicating LPN cells possess the mixed cation conductance I_H (McCormick and Pape 1990).

Many LPN neurons (33/47) showed a substantial delay in action potential firing in response to a depolarizing current step (Fig. 3, *C–F*). These delays were voltage dependent and brought about by an outward rectification during strong membrane depolarization. Figure 3*E* shows the latency (L) in firing varied with the intensity of injected current and could be fitted to an exponential decay curve ($r = 0.93$). These delays in firing were abolished by the local application of 4-AP ($n = 4$; Fig.

3*F*), suggesting they are mediated by the transient K$^+$ conductance, I_A (McCormick 1991).

Repetitive firing properties of LPN cells

LPN cells exhibited some repetitive firing properties that were distinct from first-order relay neurons. Examples of the firing patterns of LPN neurons are shown in Fig. 4. One group of cells ($n = 71$) responded to depolarizing current pulses with a steady train of action potentials and a firing frequency that varied linearly with membrane depolarization (Fig. 4*A*). We refer to this form of firing as a "regular spiking" (RS) mode. Firing frequency by current injection plots for RS cells have relatively steep slopes and a large linear operating range (Fig. 4*C*). These features can in part be attributed to the lack of spike frequency adaptation in their spike trains. Figure 4*E* shows the interspike intervals for RS cells remained relatively constant with the passage of each spike in a train at different levels of membrane depolarization.

Another group of LPN cells ($n = 23$) exhibited what we refer to as a "clustered spiking" (CS) firing mode in which
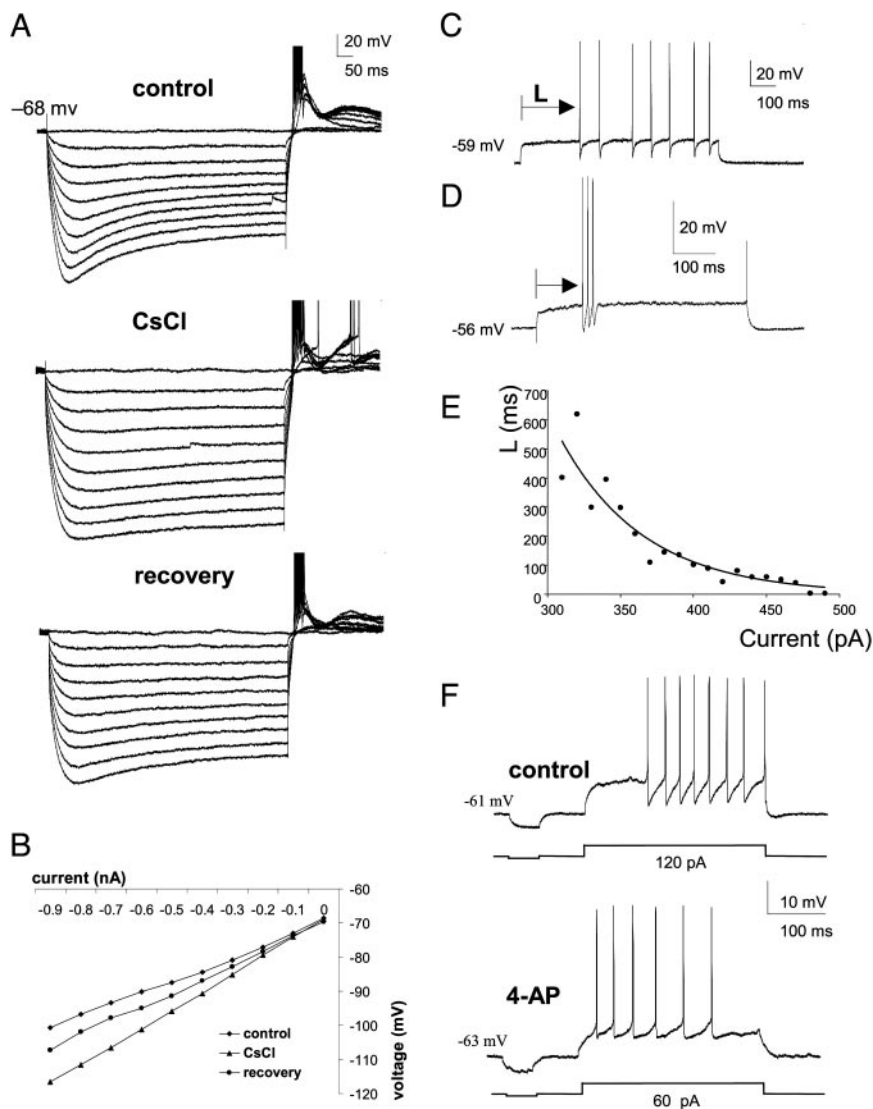
FIG. 3. Activation of the mixed cation conductance I_H and delayed spike firing in LPN relay cells. *A*: voltage responses of LPN cell recorded before (control), during, and after (recovery) the bath application of Cs^+ (2 mM). During control responses, membrane hypepolarization activates a strong inward rectifying response. This depolarizing sag was blocked by Cs^+, suggesting this response is mediated by the mixed cation conductance I_H. The depolarizing sag during membrane hyperpolarization recovers during wash-off. *B*: plot showing the degree of inward rectification associated with I_H. Membrane potentials were measured 20 ms before the end of the current pulse. *C* and *D*: examples of LPN cells showing a substantial delay in firing in response to a depolarizing current pulse. *E*: a plot showing the latency to spike firing (L) against injected current for the cell in *C*. These values could be fitted to an exponential decay curve ($r = 0.93$). *F*: responses to depolarizing current pulses before (control) and after the local application of 4-aminopyrindine (4-AP, 500 μM). In the control response, depolarization leads to a large delay in spike firing. This delay is reduced by 4-AP, indicating the involvement of the K^+ conductance I_A.

depolarizing current pulses evoked epochs of high-frequency spike discharges (Fig. 4*B*). These intermittent clustered discharges were separate and distinct from those that ride the peak of LT Ca^{2+} spikes (Fig. 5, *A* and *B*), and the firing rates of these clusters (~100 Hz) were lower than the firing frequency of bursts associated with LT Ca^{2+} spikes (~400 Hz). Firing-frequency plots reveal that CS cells responded in a nonlinear manner with firing rates that increased either quadratically (Fig. 4*D*) or exponentially (not shown) with membrane depolarization. This increase in firing rates resulted from an increase in the number of clusters and/or an increase in the number of spikes within a cluster. As illustrated in Fig. 4*F*, CS cells displayed a form of spike-frequency adaptation. Although the firing frequency within the first cluster remained relatively constant, there was an increase in the interspike interval of subsequent clusters.

When hyperpolarized to levels more negative than −65mV, depolarizing current pulses evoked LT bursts in both RS and CS cells (Fig. 5, *A* and *B*). However, when larger (sustained) current pulses were applied to hyperpolarized RS and CS cells, their responses were distinct. In this situation, LT bursts were followed by RS or CS firing respectively (Fig. 5, *C* and *D*).

We noted two measures that were correlated with the different firing modes. First, the half-width of the action potential (duration measured at half-amplitude) was greater for CS cells (mean: 1.21 ms) than for RS cells (mean: 0.73 ms). Second, the afterhyperpolarization potential (AHP) duration for RS cells (mean: 56.72 ms) was greater than that of CS cells (mean: 15.74 ms). These differences are illustrated in Fig. 6, which plots the duration of AHPs against the half-width of action potentials for RS and CS cells.

Further examination of the AHPs of RS and CS cells revealed heterogeneity that could be distinguished in part by their duration and underlying pharmacology. As illustrated in Fig. 7, *A–D*, RS cells showed the most variable AHPs. Some RS neurons displayed a very slow AHP (Fig. 7, *A–C*), lasting 87.0 ± 21.2 ms ($n = 13$), which corresponds to previous descriptions of a medium AHP (mAHP) (Sah 1996; Stocker et al. 1999). AHPs of this length have not been reported in LGN relay neurons (Deschênes et al. 1984; Williams et al., 1996). As illustrated in Fig. 7, *B* and *C,* the AHP of some RS neurons appeared to have fast and slow components that were separated by a small afterdepolarization. For other RS cells, we observed a single AHP of more intermediate length (iAHP, Fig. 7*D*)
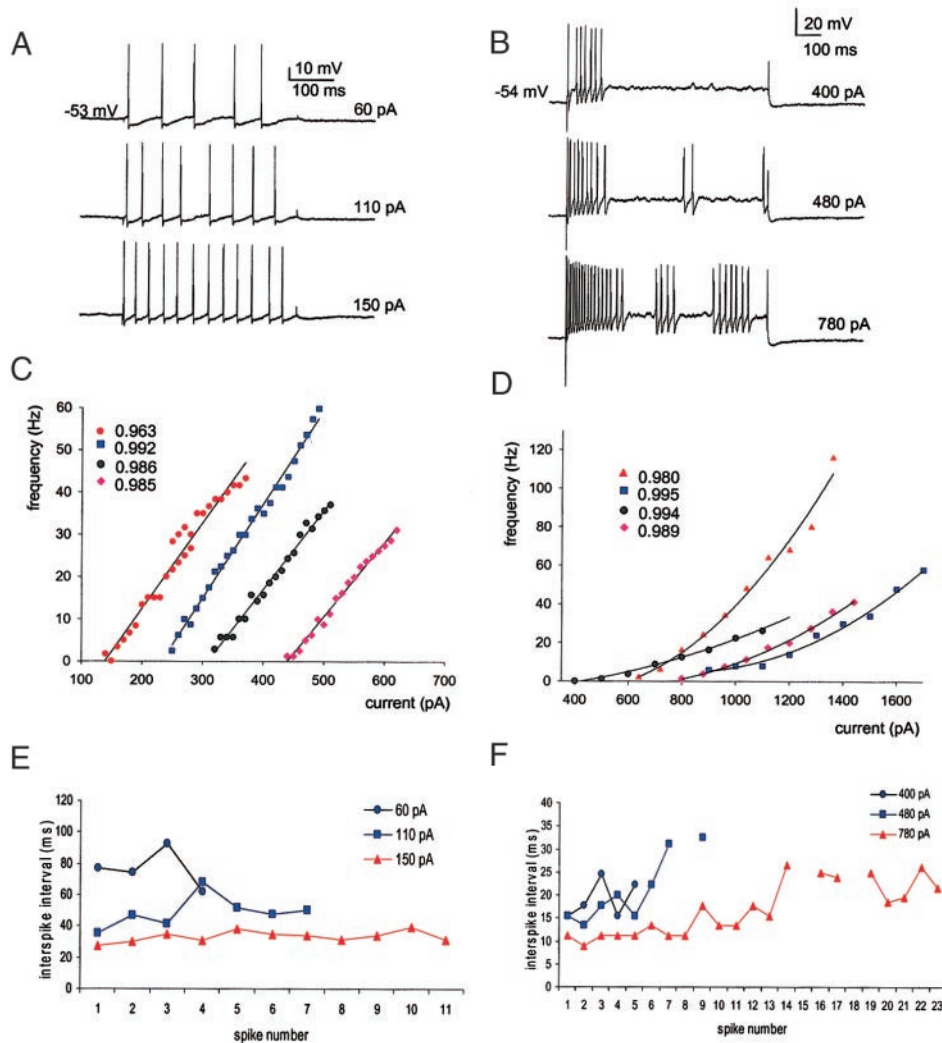
FIG. 4. Firing modes of LPN relay neurons. *A*: example of a cell that responds to depolarizing current pulses with a steady train of action potentials or in a "regular spiking" (RS) mode. Shown are the voltage responses to different depolarizing current pulses. *B*: example of a cell that responds to depolarizing current pulses in a clustered firing (CS) mode. Shown are the voltage responses to different depolarizing current pulses. *C*: examples of firing frequency by current injection plots for 4 different RS cells. In each case, the firing frequency of RS cells varies linearly with membrane depolarization. *D*: examples of firing frequency by current injection plots for 4 different CS cells. Firing frequency varies nonlinearly (quadratically) with membrane depolarization. —, regression lines and numbers depict the corresponding *r* values. *E*: interspike interval plots for the cell illustrated in *A* reveal an absence of spike frequency accommodation. *F*: interspike interval plots for the cell illustrated in *B* reveal that the firing frequency within the 1st cluster remains relatively constant, but subsequent clusters show some spike frequency accommodation.
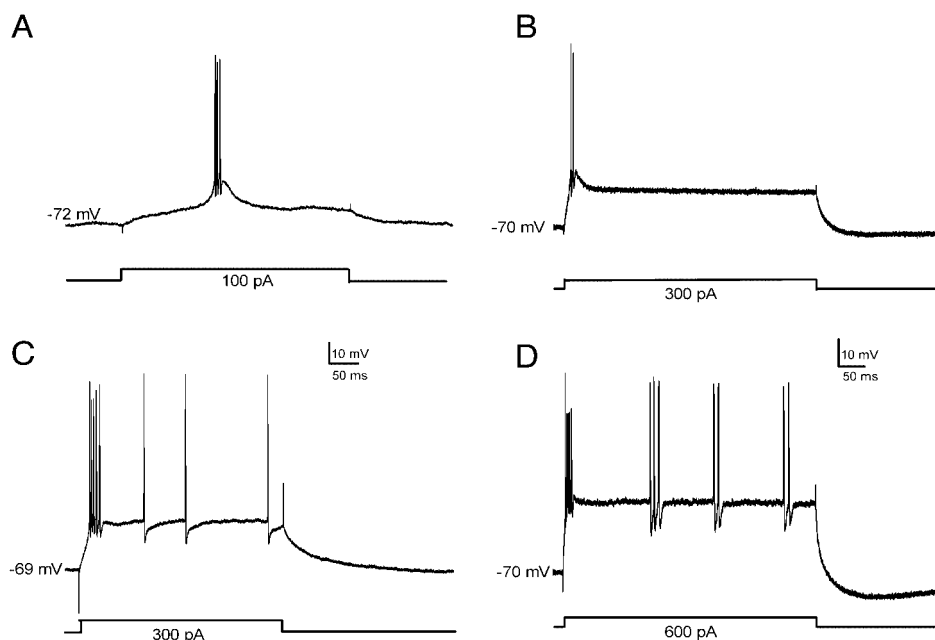

FIG. 5. Low-threshold (LT) spikes and burst firing in RS and CS cells. Membrane depolarization from a hyperpolarized state evokes LT spikes and burst discharges in RS (*A* and *C*) and CS (*B* and *D*) cells. When larger current pulses are applied, LT bursts are followed by RS (*C*) and CS firing (*D*).
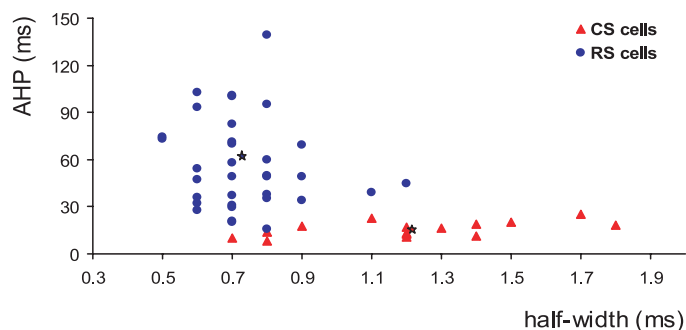
FIG. 6. The relationship between afterhyperpolarization (AHP) duration and spike half-width for RS and CS cells. The plot illustrates that RS and CS cells can be distinguished on the basis of their AHP duration and the half-width of action potential duration. RS cells (blue circles) have longer AHPs and shorter action potentials than CS cells (red triangles). Stars depict mean values.

which lasted 38.0 ± 11.6 ms ($n = 21$). As indicated in Table 1 and Fig. 7E, CS cells had the fastest AHP (fAHP) we observed that lasted 15.7 ± 4.9 ms ($n = 15$).

We investigated the conductances underlying these AHPs by applying various K^+ channel antagonists. The results of these experiments are summarized in Fig. 7, F–H. The nonspecific K^+ channel blocker, TEA significantly reduced ($P < 0.001$) the amplitude of the fAHP (Fig. 6F, 10.0 ± 1.7 to 7.3 ± 2.3 mV, a 27% reduction, $n = 4$). TEA also widened the action potential (half-width from 1.0 ± 0.2 to 2.5 ± 2.1 ms, $n = 4$, $P < 0.001$). Another nonspecific K^+ channel blocker, 4-AP, was more effective in reducing the amplitude of the fAHP (8.2 ± 2.9 to 4.2 ± 1.8 mV, a 49% reduction, $n = 5$, $P < 0.001$) and did not affect action potential width (Fig. 7G). Finally, the small-conductance calcium-activated K^+ channel blocker, apamin, reduced the amplitude and duration of the mAHP (111 ± 24 to 59 ± 13 ms, $n = 3$, $P < 0.001$) while leaving the width of the action potential and the amplitude of the fAHP intact (Fig. 7H). These results suggest that the variety in the duration of the AHPs recorded in LPN neurons can be attributed to the presence of several different potassium channels.
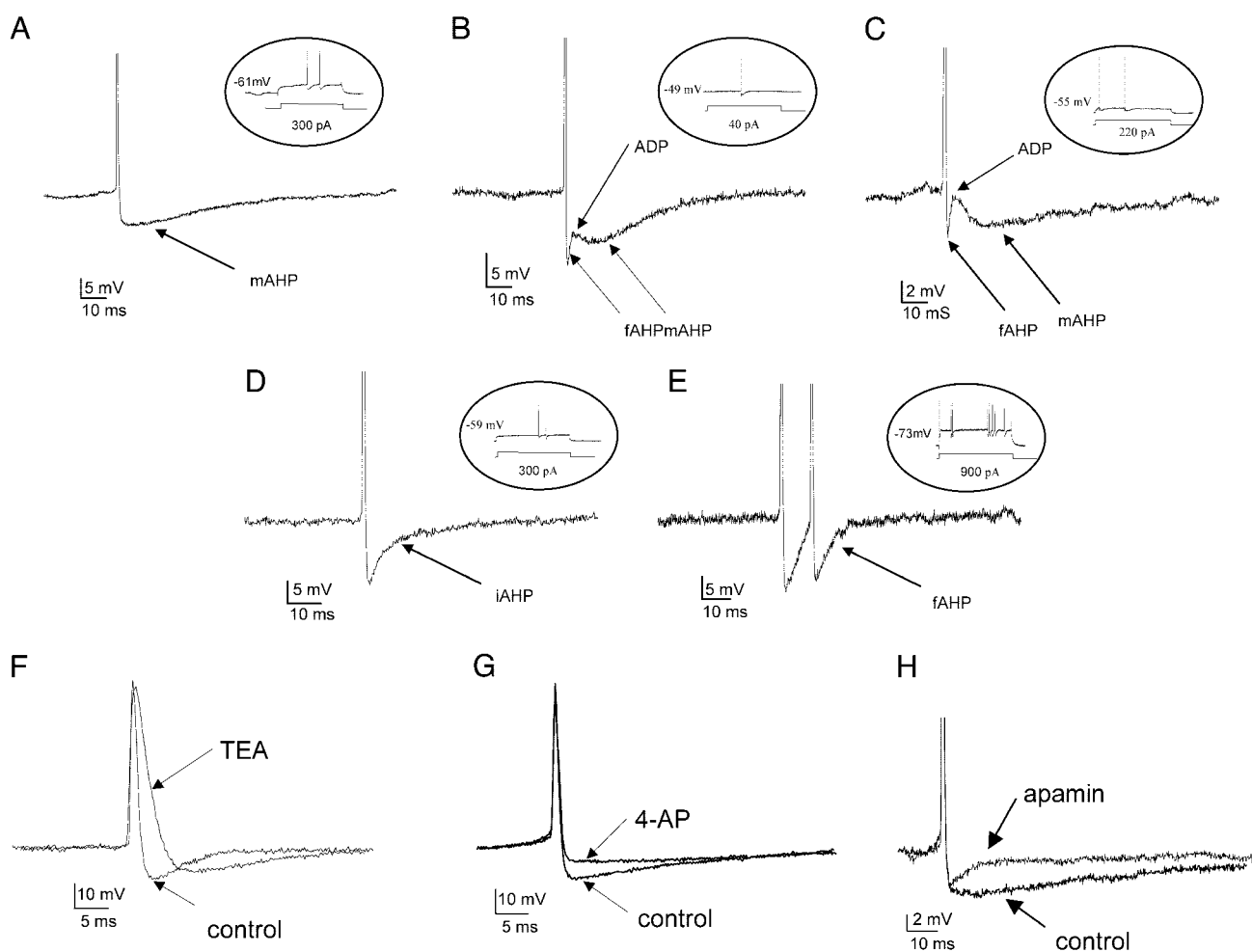

FIG. 7. AHP responses in LPN relay neurons. Shown are examples of medium AHP (mAHP, A–C), intermediate AHP (iAHP, D), and fast AHP (fAHP, E) that follows the action potential. Some neurons (B and C) exhibit both a mAHP and a fAHP that was separated by a small afterdepolarization. Insets: corresponding responses on a compressed time scale. F–H: pharmacology of AHP responses in LPN relay cells. Each panel shows a pair of superimposed responses obtained before (control) and after the application of a K^+ channel antagonist. F: example showing the nonspecific K^+ channel blocker tetraethylammonium (TEA, 10 mM, local application) widens the action potential and reduces the amplitude of the fAHP. G: example showing the nonspecific K^+ channel blocker, 4-AP is more effective in reducing the amplitude of the fAHP and does not affect action potential width. H: the small-conductance calcium-activated K^+ channel blocker, apamin, reduces the amplitude and duration of the mAHP and does not affect action potential width or the amplitude of the fAHP.

TABLE 1. *A comparison of membrane properties for CS, RS_m and RS_i cells*

	n	Resting Membrane Potential, mV	Input Resistance, MΩ	Amplitude of Action Potential, mV	Half-Width of Action Potential, ms	Duration of AHP, ms	I_A
CS cell	15	−59.5 ± 4.3	42.9 ± 12.9	60.4 ± 5.4	1.2 ± 0.3*	15.7 ± 4.9*	73%
RS_m cell	13	−57.5 ± 2.7	49.6 ± 14.6	67.7 ± 7.0	0.7 ± 0.1*	87.0 ± 21.2*	54%
RS_i cell	19	−61.6 ± 3.8	61.3 ± 21.4	65.2 ± 7.2	0.7 ± 0.2*	37.5 ± 12.1*	79%

* Significant differences in afterhyperpolarizations (AHPs) for regular spiking (RS) cells with intermediate (RS_i) and medium (RS_m) AHP and cluster spiking (CS) (t-test, $P < 0.001$) and for the half-width of the action potential for both groups of RS cells and CS cells (t-test, $P < 0.001$).

Distribution and morphology of recorded LPN neurons

We then examined the firing characteristics of LPN neurons in relation to their location in LPN. In the rodent LPN, rostral regions receive input from the cortex and caudal regions receive input from the superior colliculus (Li and Bickford 2001; Li et al. 2003; Mason and Groos 1981; Takahashi 1985). In experiments carried out in coronal slices, we noted that RS cells tended to be located in more caudal levels of the LPN, whereas CS cells seemed to be located in more rostral regions. However, this trend was difficult to quantify in brains cut in the coronal plane. To confirm that RS and CS cells are segregated in the LPN, we did experiments in slices cut in the parasagittal plane. A typical experiment is illustrated in Fig. 8. We found that CS cells were located exclusively in the rostral LPN (Fig. 8, red symbols), whereas RS cells were dispersed throughout the rostrocaudal extent of the LPN (Fig. 8, yellow and green symbols). On closer examination, we found that cells firing in the RS mode could be further subdivided by correlating their rostral-caudal location with the duration of their AHPs. RS cells with a medium AHP (>60 ms; RS_m, $n = 32$) were located only in the caudal LPN (Fig. 8, green symbols), while RS cells with an intermediate AHP (<60 ms; RS_i, $n = 39$) were more dispersed throughout the LPN (Fig. 8, yellow symbols).

With cells divided into three categories, we re-examined their membrane properties and these are summarized in Table 1. The AHPs for RS_i, RS_m, and CS cells differed significantly from each other (t-test, $P < 0.001$). The half-width of the action potential also differed between both groups of RS cells and CS cells (t-test, $P < 0.001$). However, there were no significant differences in the resting membrane potential, input resistance, or amplitude of action potentials among any of the groups. Moreover, all cells exhibited I_T and I_H and the majority of cells within each group displayed I_A (54–79%, see Table 1 and Fig. 3, C and E). We also failed to detect any consistent correlation between the firing characteristics and morphology of LPN neurons. Figure 8 provides examples of camera lucida drawings of a biocytin filled CS (Fig. 8A), RS_i (Fig. 8B), and RS_m (Fig. 8C) cell. While there is an inherent variability in dendritic morphology among these cells, they are indistinguishable from class A thalamocortical relay cells (Grossman et al. 1973).
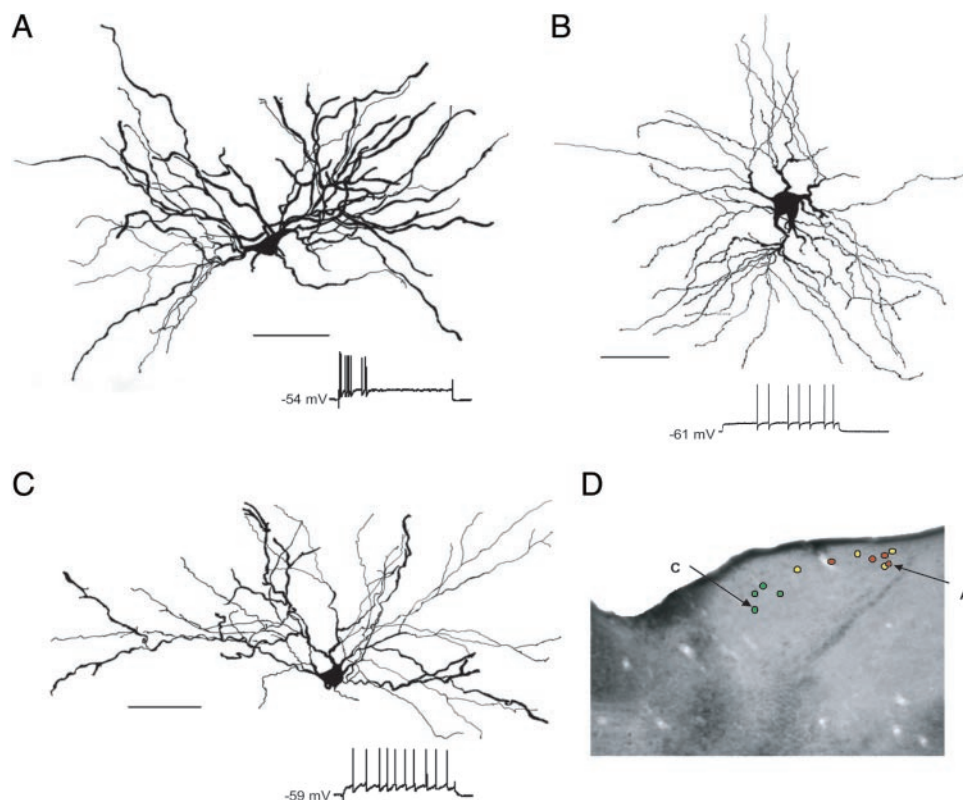

FIG. 8. Morphology and distribution of RS and CS cells in the LPN. Camera lucida reconstructions of LPN relay cells filled with biocytin during the recording. Beneath each cell is a corresponding voltage response showing the cell's firing mode. A: an example of a CS cell. B: an example of an RS_i cell. C: an example of an RS_m cell. D: example of a parasagittal slice showing the location and distribution of recorded CS and RS cells in a typical experiment. CS cells (red dots) are located in the rostral LPN. RS cells with medium AHPs (RS_m, green dots) are located in the caudal LPN. RS cells with intermediate AHPs (RS_i cells, yellow dots) are more dispersed. The location of the cells illustrated in A and B are indicated by arrows. Scale bars = 50 μm.

DISCUSSION

The present report provides the first detailed description of the functional properties of relay neurons in the LPN, a proposed higher-order nucleus. We found that relay neurons of the LPN possess many of the same voltage-gated conductances that have been reported for first-order relay neurons of the LGN. Most notable was the presence of the mixed cation conductance I_H and the LT T-type Ca^{2+} conductance that underlies burst firing. In the LGN, the interplay of these conductances with GABAergic inhibition originating from the thalamic reticular nucleus (TRN) promotes intrinsic oscillatory activity that occurs during certain behavioral or pathological states (McCormick and Bal 1997). It has previously been shown that the synaptic targets of TRN terminals are similar in first- and higher-order nuclei (Wang et al. 2001). These results taken together with the present report suggest that higher-order thalamic relay neurons can engage in rhythmic events similar to those described in first-order nuclei, and thus contribute to the widespread distribution of thalamic oscillatory activity.

Despite these similarities, we did note that the repetitive firing characteristics of higher-order LPN relay neurons differed from first-order LGN relay neurons. We found that cells in the LPN fired linearly in a RS mode or nonlinearly with epochs of high-frequency bursts in a CS mode. The bursting associated with the CS mode differs from the conventional LT Ca^{2+} mediated burst mode of thalamic relay neurons. While both forms of bursting are highly nonlinear, their temporal patterning and voltage dependency differ substantially (McCormick and Feeser 1990).

The RS mode of LPN relay neurons also differs from the tonic mode of LGN neurons. Firing frequency by current injection plots for regular spiking cells are steeper and exhibit a much larger linear operating range (McCormick and Feeser 1990; Zhan et al. 1999). The tonic firing of LGN neurons also shows substantial spike frequency adaptation (Smith et al. 2001; Zhan et al. 1999), a feature that was not apparent in the regular spiking of LPN neurons. These differences may be attributed to the relative strength and density of various K^+ conductances involved in the regulation of the f- and mAHPs of thalamic relay cells.

Previous studies have noted that LGN interneurons display longer AHPs than LGN relay cells (Williams et al. 1996). The AHPs of interneurons are similar in some ways to the AHPs of the RS cells. However, in the LPN we did not observe the slow voltage ramp that occurs prior to the start of each action potential. In addition, the duration of action potentials for LPN cells was greater than those of interneurons. Similarly, the responses of LPN CS cells are reminiscent of the responses of "fast spiking" cortical interneurons (Kawaguichi 1995; McCormick et al. 1985). However, the width of the action potentials of CS cells is wider than that of parvalbumin-containing fast-spiking interneurons (Galarreta and Hestrin 2002) and no neurons in the LPN stain for parvalbumin (see Fig. 1).

The response profile of CS cells in the rodent LPN more closely resembles the firing mode of relay cells in the dorsolateral nucleus of the avian thalamus (Luo and Perkel 2002). In addition, responses similar to CS LPN neurons have been recorded in relay cells located within the shell region of the cat ventroposterior lateral nucleus (VPL) (Turner et al. 1997).

Because responses similar to CS cells have not been recorded in well-characterized first-order thalamic nuclei such as the rat LGN (Crunelli et al. 1987; Williams et al. 1996) or ventrobasal complex (Velazquez and Carlen 1996), it raises the possibility that the rat LPN and the shell region of the cat VPL share properties distinct from first order nuclei. Some areas of the primate VPL are innervated by two types of cortical terminals (Darian-Smith et al. 1999) and thus might be considered higher order (Guillery 1995). However, this information is unavailable for the cat VPL. At this point, we can confidently state that within the rat visual thalamus, the firing properties of higher-order relay neurons are distinct from those of first-order relay neurons. Whether this distinction will hold true for thalamic nuclei representing other sensory modalities, or indeed whether the first-order/higher-order distinction applies to all thalamic regions, requires further investigation.

We are also confident that the LPN cell responses that we observed were recorded from relay cells rather than interneurons. First, all of our biocytin-filled cells were larger than GABAergic interneurons. Second, their dendritic morphology was consistent with that of first order thalamocortical cells. Finally, we previously noted that GABAergic interneurons in the LPN are much sparser than in the LGN, and are virtually absent in the rostral LPN (Li et al. 2003).

This lack of interneurons in the rostral LPN is worth noting because this is the region where CS cells are concentrated. The rostral LPN also receives dense input from the visual cortex (Li et al. 2003; Mason and Groos 1981; Takahashi 1985). This includes inputs from cortical layer V cells that do not project to first-order thalamic nuclei but do provide large "driver-like" inputs to higher-order nuclei (Guillery and Sherman 2002) such as the LPN (Bourassa and Deschênes 1995; Li et al. 2003). Higher-order nuclei of the visual thalamus project densely to cortical layer I (Abramson and Chalupa 1985), where the apical dendrites of layer V cells end in tufts (Klein et al. 1986). Thus the high-frequency bursts of CS cells could be particularly effective in activating layer V cells (Swadlow and Gusev 2001; Thomson 2000). It is possible that the response characteristics of CS cells are important for strengthening and maintaining cortico-thalamo-cortical signals through the rostral LPN.

In contrast, RS cells are located in more caudal levels of the LPN. In particular, RS cells with the slowest AHPs (RS_m cells) are clustered in the most caudal LPN. This region of the LPN receives input from the retinorecipient zones of the superior colliculus (Li and Bickford 2001; Mason and Groos 1981; Takahashi 1985). In fact, the firing characteristics of RS_m cells are similar to the firing characteristics of tectothalamic cells (Lo et al. 1998). Such firing may be important for the accurate transfer of these signals through the caudal LPN to the cortex and/or striatum (Takada 1992). Thus in the LPN, RS and CS cells may be driven by subcortical and cortical inputs, respectively, and the distinct temporal properties of their response modes may be a necessary component of circuits that are unique to higher-order nuclei.

REFERENCES

Abramson BP and Chalupa LM. Multiple pathways from the superior colliculus to the extrageniculate visual thalamus of the cat. *J Comp Neurol* 15: 397–418, 1985.

Bourassa J and Deschênes M. Corticothalamic projections from the primary visual cortex in rats: a single fiber study using biocytin as anterograde tracer. *Neuroscience* 66: 253–263, 1995.

Crunelli V, Kelly JS, Leresche N, and Pirchio M. The ventral and dorsal lateral geniculate nucleus of the rat: intracellular recordings in vitro. *J Physiol* 384: 587–601, 1987.

Deschênes M, Paradis M, Roy JP, and Steriade M. Electrophysiology of neurons of lateral thalamic nuclei in cat: resting properties and burst discharges. *J Neurophysiol* 51: 1196–1219, 1984.

Darian-Smith C, Tan A, and Edwards S. Comparing thalamocortical and corticothalamic microstructure and saptial reciprocity in the macaque ventral posterolateral nucleus (VPLc) and medical pulvinar. *J Comp Neurol* 410: 211–234, 1999.

Galarreta M and Hestrin S. Electrical and chemical synapses among parvalbumin fast-spiking GABAergic interneurons in adult mouse neocortex. *Proc Natl Acad Sci USA* 99: 12438–12443, 2002.

Grossman A, Lieberman AR, and Webster KE. A Golgi study of the rat lateral geniculate nucleus. *J Comp Neurol* 150: 441–446, 1973.

Guido W, Gunhan-Agar E, and Erzurumlu RS. Developmental changes in the electrophysiological properties of brain stem trigeminal neurons during pattern (barrelette) formation. *J Neurophysiol* 79: 1295–1306, 1998.

Guido W, Lo FS, and Erzurumlu RS. An in vitro model of the kitten retinogeniculate pathway. *J Neurophysiol* 77: 511–516, 1997.

Guillery RW. Anatomical evidence concerning the role of the thalamus in corticocortical communication: a brief review. *J Anat (Lond)* 187: 583–592, 1995.

Guillery RW and Sherman SM. Thalamic relay functions and their role in corticocortical communication: generalizations from the visual system. *Neuron* 33: 163–175, 2002.

Hernandez-Cruz A and Pape HC. Identification of two calcium currents in acutely dissociated neurons from the rat lateral geniculate nucleus. *J Neurophysiol* 61: 1270–1283.

Horikawa K and Armstrong WE. A versatile means of intracellular labeling: injection of biocytin and its detection with avidin conjugates. *J Neurosci Methods* 25: 1–11, 1988.

Hu B. Membrane potential oscillations and corticothalamic connectivity in rat associational thalamic neurons in vitro. *Acta Physiol Scan* 148: 109–113, 1993.

Kawaguchi Y. Physiological subgroups of nonpyramidal cells with specific morphological characteristics in layer II/III of rat frontal cortex. *J Neurosci* 15: 2638–2655, 1995.

Klein BG, Mooney RD, Fish SE, and Rhoades RW. The structural and functional characteristics of striate cortical neurons that innervate the superior colliculus and lateral posterior nucleus in hamster. *Neuroscience* 17: 57–78, 1986.

Li J and Bickford ME. Synaptic targets of tectothalamic terminals in the rat lateral posterior nucleus. *Soc Neurosci Abstr* 27: 723.25, 2001.

Li J, Wang S, and Bickford, ME. A comparison of the ultrastructure of cortical and retinal inputs in the rat dorsal lateral geniculate and lateral posterior nuclei. *J Comp Neurol* 460: 394–409, 2003.

Lo FS, Cork RJ, and Mize RR. Physiological properties of neurons in the optic layers of the rat's superior colliculus *J Neurophysiol* 80: 331–334, 1998.

Luo M and Perkel DJ. Intrinsic and synaptic properties of neurons in an avian thalamic nucleus during song bird learning. *J Neurophysiol* 88: 1903–1914, 2002.

Mason R and Groos GA. Cortico-recipient and tecto-recipient visual zones in the rat's lateral posterior (pulvinar) nucleus: an anatomical study. *Neurosci Lett* 25: 107–112, 1981.

McCormick DA. Functional properties of a slowly inactivating postassium current in guinea pig dorsal lateral geniculate relay neurons. *J Neurophysiol* 66: 1176–1189, 1991.

McCormick DA. Neurotransmitter actions in the thalamus and cerebral cortex and their role in neuromodulation of thalamocortical activity. *Prog Neurobiol* 39: 337–388, 1992.

McCormick DA and Bal. Sleep and arousal: thalamocortical mechanisms. *Annu Rev Neurosci* 20: 185–215, 1997.

McCormick DA, Conners BW, Lighthall JW, and Prince DA. Comparative electrophysiology of pyramidal and sparsely spiny stellate neurons of neocortex. *J Neurophysiol* 54: 782–806, 1985.

McCormick DA and Feeser HR. Functional implications of burst firing and single spike activity in lateral geniculate relay neurons. *Neuroscience* 39: 103–113, 1990.

McCormick DA and Pape HC. Properties of hyperpolarization-activated cation current and its role in rhythmic oscillation in thalamic relay neurons. *J Physiol* 431: 319–342, 1990.

Monckton JE and McCormick DA. Neuromodulatory role of serotonin in the ferret thalamus. *J Neurophysiol* 87: 2124–2136, 2002.

Montero VM and Zempel J. Evidence for two types of GABA-containing interneurons in the A-laminae of the cat lateral geniculate nucleus: a double-label HRP and GABA-immunocytochemical study. *Exp Brain Res* 60: 603–609, 1985.

Ralston HJ 3rd and Herman MM. The fine structure and synapses in ventrobasal thalamus of the cat. *Brain Res* 14: 77097, 1969.

Sah P. Ca^{2+}-activated K^+ currents in neurons: types, physiological roles and modulation. *Trends Neurosci* 19: 150–154, 1996.

Sherman SM. Tonic and burst firing: dual modes of thalamocortical relay. *Trends Neurosci* 24: 122–126, 2001.

Smith GD, Cox CL, Sherman SM, and Rinzel J. A firing model of spike frequency adaptation in sinusoidally driven thalamocortical relay neurons. *Thalamus Related Syst* 11: 1–22, 2001.

Stocker M, Krause M, and Pedarzani P. An apamin-sensitive Ca^{2+}-activated K^+ currrent in hippocampal pyramidal neurons. *Proc Natl Acad Sci USA* 96: 4662–4667, 1999.

Steriade M and Llinás R. (1988) The functional states of thalamus and the associated neuronal interplay. *Physiol Rev* 68: 649–742, 1988.

Swadlow HA and Gusev AG. The impact of "bursting" thalamic impulses at a neocortical synapse. *Nat Neurosci* 4: 402–412, 2001.

Takada M. The lateroposterior thalamic nucleus and substantia nigra pars lateralis: origin of dual innervation over the visual system and basal ganglia. *Neurosci Lett* 139: 153–156, 1992.

Takahashi T. The organization of the lateral thalamus of the hooded rat. *J Comp Neurol* 231: 281–309, 1985.

Thomson AM. Facilitation, augmentation, and potentiation at central synapses. *Trends Neurosci* 23: 305–312, 2000.

Turner JP, Anderson CM, Williams SR, and Crunelli V. Morphology and membrane properties of neurons in the cat ventrobasal thalamus in vitro. *J Physiol* 505: 707–726, 1997.

Velazquez JLP and Carlen PL. Development of firing patterns and electrical properties in neurons of the rat ventrobasal thalamus. *Dev Brain Res* 91: 164–170, 1996.

Wang S, Bickford ME, Van Horn SC, Erisir A, Godwin DW, and Sherman SM. Synaptic targets of thalamic reticular nucleus terminals in the visual thalamus of the cat. *J Comp Neurol* 440: 321–341, 2001.

Webster MJ and Rowe MH. Morphology of identified relay cells and interneurons in the dorsal lateral geniculate nucleus of the rat. *Exp Brain Res* 56: 468–474, 1984.

Williams SR, Turner JP, Anderson CM, and Crunelli V. Electrophysiological and morphological properties of interneurons in the rat dorsal lateral geniculate nucleus. *J Physiol* 490: 129–147, 1996.

Zhan XJ, Cox CL, Rinzel J, and Sherman SM. Current-clamp and modeling studies of low-threshold calcium spikes in cells of the cat's lateral geniculate nucleus. *J Neurophysiol* 81: 2360–2373, 1999.

Zhu JJ and Heggleund P. Muscarinic regulation of dendritic and axonal outputs of rat thalamic interneurons: a new cellular mechanism for uncoupling distal dendrites. *J Neurosci* 21: 1148–1159, 2001.